Excitation of isoscalar giant monopole resonance by inelastic scattering of 240 MeV α-particles

Alexei Kolomiets, Oleksiy Pochivalov, and Shalom Shlomo
Cyclotron Institute, Texas A&M University, USA

We consider the excitation of the isoscalar giant monopole resonances (ISGMR) excitations in ^{28}Si, ^{40}Ca, ^{58}Ni, and ^{116}Sn. We carry out self-consistent Skyrme-Hartree-Fock (HF) Random Phase Approximation (RPA) calculations of the strength distributions $S(E)$ and the transition densities $\rho_{tr}(r)$ as functions of the excitation energy E. Recent experimental data of 240 MeV α-particle scattering by these nuclei is analyzed within the Distorted Wave Born Approximation (DWBA) using the folding model (FM) with a density dependent Gaussian nucleon-α interaction $V(\rho,r)$. The parameters of $V(\rho,r)$ are found by fitting the experimentally measured angular cross sections $\sigma(\theta)$ for the case of elastic scattering, using the HF ground state density ρ_{HF}. The inelastic cross sections $\sigma(\theta)$ for the ISGMR are then obtained using the FM-DWBA and both microscopic (RPA) and hydrodynamical (collective model) $\rho_{tr}(r)$ (found from $\rho_{HF}(r)$). Possible overestimation of the energy weighted sum rules and shifts of the centroid energies due to the collective-model-based DWBA reaction description are obtained.

Introduction

The study of nuclear giant resonances has long been the subject of extensive theoretical and experimental studies.[1] In this work we consider the excitation of the isoscalar giant monopole resonance (ISGMR) in several nuclei by inelastic scattering of 240 MeV α-particles and carry out a realistic microscopic analysis of recent and highly accurate experimental data. Determination of the parameters describing ISGMR excitation in both heavy and light nuclei is a topic of current interest. The interest is stimulated mainly by the possibility of extracting the value of nuclear matter incompressibility coefficient (which is important for studies of nuclear equation of state, neutron stars, supernovae explosion and heavy ion reactions[2]) from the knowledge of ISGMR strength distributions and centroid energies in nuclei throughout the periodic table.[3–6]

Recently, experimental studies of giant resonance excitations in nuclei ranging from ^{12}C to ^{208}Pb were performed at Texas A&M University using 240 MeV bombarding energy α-particles.[7–10] Excellent peak-to-continuum ratios in the observed inelastic scattering spectra were obtained and the ambiguity associated with the continuum subtraction was notably reduced. New conclusions regarding isoscalar monopole strength distributions in some $A < 90$ nuclei have been drawn.[8,9]

On the one hand, it is interesting to compare the new experimental data with the theoretical predictions based on self-consistent Hartree-Fock (HF) Random Phase Approximation (RPA) calculations with zero-range Skyrme-type interactions. On the other hand, it is important to investigate the consequences of some assumptions made in the experimental analysis itself. In particular, it is a common practice in experimental studies to assume the collective model radial shapes of transition densities. This assumption needs to be carefully examined, especially for light nuclei since, as was reported in Ref. 11, it may lead to the overestimation of the isoscalar monopole (E0T0) energy weighted sum rule (EWSR) by up to 30%.

The purpose of this talk is two-fold. First, we give a full microscopic description of isoscalar monopole excitations in ^{28}Si, ^{40}Ca, ^{58}Ni, and ^{116}Sn based on self-consistent HF-RPA calculations. We use the SL1 parametrization of the Skyrme interaction[12] which gives the value of nuclear matter incompressibility of 230 MeV. Second, we give a theoretical description of 240 MeV α-particle scattering reactions within the folding model Distorted Wave Born Approximation (DWBA) and compare our HF-RPA results with the conclusions drawn from the experimental-like analysis of cross sections. We investigate how the approximate form of the isoscalar monopole (E0T0) transition density deduced from the collective model may affect the results regarding the strengths and excitation energies of E0T0 resonances.

Hartree-Fock-Random-Phase-Approximation formalism

The delta-functional coordinate dependence of the Skyrme interaction makes it possible to give a simplified coordinate space formulation of the RPA in terms of Green's functions.[13] The RPA Green's function $G^{RPA}(\mathbf{r},\mathbf{r}',E)$ is found from the equation

$$\begin{aligned} G^{RPA}(\mathbf{r},\mathbf{r}',E) &= G^0(\mathbf{r},\mathbf{r}',E) \\ &\quad + \int d\mathbf{r}_1 d\mathbf{r}_2\, G^0(\mathbf{r},\mathbf{r}_1,E) \\ &\quad \cdot V_{ph}(\mathbf{r}_1,\mathbf{r}_2) G^{RPA}(\mathbf{r}_2,\mathbf{r}',E), \end{aligned} \tag{1}$$

where $G^0(\mathbf{r},\mathbf{r}',E)$ is the Green's function of the free system and $V_{ph}(\mathbf{r}_1,\mathbf{r}_2)$ is the zero-range particle-hole interaction.

In order to be able to consider both closed-shell and open-shell nuclei, we follow the ansatz proposed in Ref. 14 and evaluate the free-system Green's function from

$$\begin{aligned} G^0(\mathbf{r},\mathbf{r}',E) = \sum_{p,h} \theta_h(1-\theta_p) \cdot \Bigg[& \frac{\phi_p(\mathbf{r})\phi_h^*(\mathbf{r})\phi_p^*(\mathbf{r}')\phi_h(\mathbf{r}')}{E-\varepsilon_p+\varepsilon_h+i\Gamma/2} \\ & - \frac{\phi_h(\mathbf{r})\phi_p^*(\mathbf{r})\phi_h^*(\mathbf{r}')\phi_p(\mathbf{r}')}{E+\varepsilon_p-\varepsilon_h+i\Gamma/2} \Bigg], \end{aligned} \tag{2}$$

where $\phi_k(\mathbf{r})$ and ε_k are the Hartree-Fock single-particle wave functions and energies, $\Gamma/2$ is the smearing half-width, θ_h and θ_p are the occupation numbers of the Hartree-Fock single-particle states, and the summation over p and h states is extended to the entire single-particle spectrum. For a spherically symmetric nucleus, the occupation numbers can be taken simply as $\theta_\lambda = N_\lambda/(2j_\lambda+1)$, where N_λ and j_λ are the number of nucleons on the single-particle orbital λ and their angular momentum, respectively. The expression for $V_{ph}(\mathbf{r}_1,\mathbf{r}_2)$ in terms of Skyrme-force parameters can be found elsewhere[13,15,16]

The quantities characterizing nuclear excitations can easily be found using the RPA Green's function. In particular, the transition strength distribution $S(E)$ and its energy moments M_k for the one-body excitation operator $Q = \sum_{i=1}^{A} f(\mathbf{r}_i)$ are obtained from

$$S(E) = -\frac{1}{\pi}\int d\mathbf{r}d\mathbf{r}'\mathrm{f}^*(\mathbf{r})\mathrm{Im}\left[\mathrm{G}^{\mathrm{RPA}}(\mathbf{r},\mathbf{r}',\mathrm{E})\right]\mathrm{f}(\mathbf{r}'), \qquad (3)$$

$$M_k = \int_0^\infty d\,E\mathrm{E}^{\mathrm{k}}\mathrm{S(E)} = -\frac{1}{\pi}\int \mathrm{dE}\mathrm{E}^{\mathrm{k}} \times \left[\int d\mathbf{r}d\mathbf{r}'\mathrm{f}^*(\mathbf{r})\mathrm{Im}\left[\mathrm{G}^{\mathrm{RPA}}(\mathbf{r},\mathbf{r}',\mathrm{E})\right]\mathrm{f}(\mathbf{r}')\right], \qquad (4)$$

while the transition density $\delta\rho(\mathbf{r},E_\nu)$ for the excited state $|\nu\rangle$ having the excitation energy E_ν and the half-width $\Gamma/2$ is given by

$$\delta\rho(\mathbf{r},E_\nu) = \pm\left[-\frac{\Gamma}{2}\mathrm{Im}\left(\mathrm{G}^{\mathrm{RPA}}(\mathbf{r},\mathbf{r},\mathrm{E}_\nu)\right)\right]^{\frac{1}{2}}. \qquad (5)$$

A desired feature of HF-RPA calculations is preservation of the free-system's energy weighted sum rule. It has been proven[13,17] that such a self-consistency can be achieved if: (1) the interaction used to perform the Hartree-Fock calculations is also used to obtain the particle-hole interaction, and (2) all the terms obtained as a result of evaluating expression are retained in the process of calculating the RPA Green's function from Eq. (1). In the present work we follow the stated self-consistent approach.

"Microscopic" versus "Macroscopic" description of α-scattering within the folding model DWBA

The Distorted Wave Born Approximation (DWBA) has been widely used in experimental studies in order to give a theoretical description of low-energy scattering reactions and, thus, analyze measured cross sections of scattered probes. The folding model approach[18,19] to the evaluation of optical potentials appears to be quite successful and is extensively used at present in theoretical descriptions of α-particle scattering.[20–23] This approach provides a direct link to the description of α-particle scattering reactions based on microscopic HF-RPA results.

Within the folding model approach, the optical potential $U(r)$ is given by

$$U(r) = \int d\mathbf{r}' V(|\,\mathbf{r}-\mathbf{r}'|,\rho_0(r'))\rho_0(r') \qquad (6)$$

where $V(|\,\mathbf{r}-\mathbf{r}'|,\rho_0(r'))$ is the nucleon-α interaction, which is generally complex and density dependent, and $\rho_0(r')$ is the ground state (Hartree-Fock) density of a spherical target nucleus. It is customary to adopt a certain form for the nucleon-α interaction and obtain the interaction parameters from the fit to experimentally measured elastic angular distributions. In this work, both real and imaginary parts of the nucleon-α interaction are chosen to have the Gaussian shape with density dependence

$$V(|\,\mathbf{r}-\mathbf{r}'\,|,\rho_0(r')) = V(1+\beta_V\rho_0^{2/3}(r'))e^{-\frac{|\mathbf{r}-\mathbf{r}'|^2}{\alpha_V}} + iW(1+\beta_W\rho_0^{2/3}(r'))e^{-\frac{|\mathbf{r}-\mathbf{r}'|^2}{\alpha_W}}. \qquad (7)$$

The parameters V, β_V, α_V and W, β_W, α_W in Eq. (7) are determined by a fit of the elastic scattering data. Similar form of nucleon-α interaction was used in Ref. 22 where scattering of 129 and 240 MeV α-particles by ^{58}Ni was considered.

For a state with the multipolarity L and excitation energy E, the radial form $\delta U_L(r,E)$ of the transition potential can be found from

$$\delta U(r,E) = \int d\mathbf{r}'\left[V(|\,\mathbf{r}-\mathbf{r}'\,|,\rho_0(r')) + \rho_0(r')\frac{\partial V(|\,\mathbf{r}-\mathbf{r}'\,|,\rho_0(r'))}{\partial\rho_0(r')}\delta\rho_L(\mathbf{r}',E)\right], \qquad (8)$$

where $\delta\rho_L(\mathbf{r}',E)$ is the transition density for the considered state.

At this point, we can distinguish between the microscopic and the macroscopic approaches to the α-particle scattering description based on the folding model. Within the "microscopic" approach, both the ground state density and the transition density which enter Eqs. (6) and (8) are obtained from the self-consistent Hartree-Fock-RPA calculations. Within the "macroscopic" approach, the transition densities are assumed to have energy-independent radial shapes and are obtained from the ground state density using the collective model. In particular, the so-called Tassie radial shape of the transition density[24] is used in experimental studies of isoscalar monopole resonance excitations

$$\delta\rho_{L=0}(r) = -\alpha(E)\left(3\rho_0(\mathrm{r}) + \mathrm{r}\frac{\mathrm{d}\rho_0(\mathrm{r})}{\mathrm{dr}}\right), \qquad (9)$$

where the energy-dependent factor $\alpha(E)$ is determined by fitting measured inelastic cross sections. The amount of isoscalar monopole strength concentrated in a given resonance state can then be deduced from the knowledge of $\alpha(E)$ in a straightforward manner, bearing in mind that for the state E_R that exhausts 100% of E0T0 EWSR this coefficient is given by[24]

$$\alpha^2(E_R) = 2\pi \frac{\hbar^2}{mA\langle r^2\rangle E_R} \quad (10)$$

with m, A, and $\langle r^2\rangle$ being the nucleon mass, the number of nucleons in the excited nucleus, and the ground state mean-square radius, respectively.

It is not clear that the collective model result (9) is a good approximation for the monopole transition density, especially in lighter nuclei. In the following, we test this approximation by performing folding model-DWBA analysis of α-particle scattering by several nuclei ranging from ^{28}Si to ^{116}Sn.

Results and discussion

The numerical solution of Eq. (1) using the SL1 parametrization of the Skyrme interaction[12] is the core of our microscopic calculations. The detailed description of analogous calculations can be found in the literature (see, for example, Refs. 13, 15 and 16). We obtain the E0T0 strength distributions from Eq. (3) using $Q_{00} = \frac{1}{\sqrt{4\pi}} \sum_{i=1}^{A} r_i^2$ which is the generally accepted form for the E0T0 excitation operator. The E0T0 transition densities are found from Eq. (5).

Our HF-RPA results for the E0T0 transition strength distributions in ^{28}Si, ^{40}Ca, ^{58}Ni, and ^{116}Sn nuclei are shown in Fig. 1. The resonance energies and percentages of the total E0T0 EWSR exhausted below 40 MeV excitation energy are given in Table 1 and compared to recent experimental data. A rather good agreement with the experiment was achieved for ^{28}Si and ^{40}Ca nuclei. A significant difference between the theoretical and experimental amounts of E0T0 EWSR exists in ^{58}Ni. Our microscopic results indicate that in ^{58}Ni, as well as in other considered nuclei, nearly 100% of E0T0 EWSR is present below 40 MeV excitation energy in contrast with no more than 50% reported in recent studies[7,22] based on the cross section analysis.

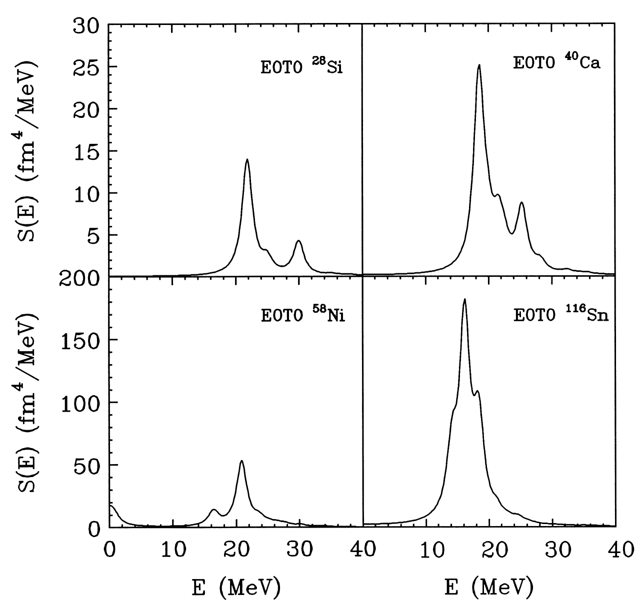

Fig. 1. Calculated ISGMR strength distributions in ^{28}Si, ^{40}Ca, ^{58}Ni, and ^{116}Sn nuclei.

Table 1. Resonance and centroid energies, and percentages of the EWSR exhausted within the energy region $10 < E < 40$ MeV for ISGMR excitation in ^{28}Si, ^{40}Ca, ^{58}Ni, and ^{116}Sn nuclei. Comparison with recent experimental data is provided.

	^{28}Si	^{40}Ca	^{58}Ni	^{116}Sn
E_R (MeV)	21.8, 30.0	18.6, 25.2	16.4, 20.8	16.2
$\frac{M_1}{M_0}$ (MeV)	24.0	21.1	21.2	17.2
Exp.	21.5[a]	18.9[b]		
$\sqrt{\frac{M_1}{M_{-1}}}$ (MeV)	23.6	20.7	20.8	16.9
Exp.	20.7[a]	17.3[b]		
$\sqrt{\frac{M_3}{M_1}}$ (MeV)	25.4	22.6	22.6	18.6
Exp.	23.7[a]	21.3[b]		
% EWSR	91	94	96	95

[a]Ref. 9, [b]Ref. 8.

At the next stage of our calculations, using Eqs. (6) and (7) and the Hartree-Fock ground state density, we construct the optical potential and determine the parameters of the nucleon-α interaction of Eq. (7) by fitting experimentally measured elastic scattering angular distributions. Numerical DWBA calculations were performed with the computer program PTOLEMY.[25] Quite satisfactory fits were obtained with

$$V(|\mathbf{r}-\mathbf{r}'|, \rho_0(r')) = -38 \text{ MeV } (1 - 1.9\text{fm}^2 \rho_0^{2/3}(\text{r}'))\text{e}^{-\frac{|\text{r}-\text{r}'|^2}{3.7\text{fm}^2}} + iW(1 - 1.9\text{fm}^2\rho_0^{2/3}(\text{r}'))\text{e}^{-\frac{|\text{r}-\text{r}'|^2}{5.1\text{fm}^2}}, \quad (11)$$

where:

$W = -11.2$ MeV for ^{28}Si and ^{58}Ni,
$W = -10.0$ MeV for ^{40}Ca,
$W = -11.4$ MeV for ^{116}Sn.

Having determined the parameters of the nucleon-α interaction, we calculate the cross sections of inelastically scattered α-particles for the case of E0T0 excitation of the target nucleus using the transition potential (8) and the RPA transition density (5) shown in Fig. 2. These cross sections serve as experimental data to be analyzed following the typical procedure based on the spectrum subtraction technique.[26] This procedure is illustrated in Fig. 3 for the case of ^{116}Sn. The middle panel of Fig. 3 shows 0° double differential E0T0 cross sections obtained with RPA transition density (i.e. our "experimental" data). In the lower panel we show the 0° E0T0 cross sections found using the transition potential (8) and the collective model E0T0 transition density (9) normalized to 100% of E0T0 EWSR (see Eq. (10)). The dashed line in the upper panel of Fig. 3 is the ratio of the curve in the middle panel and the one in the lower panel. It represents the fraction of the E0T0 EWSR per unit energy reconstructed from our "experimental" cross sections. The solid line in the upper panel shows the actual

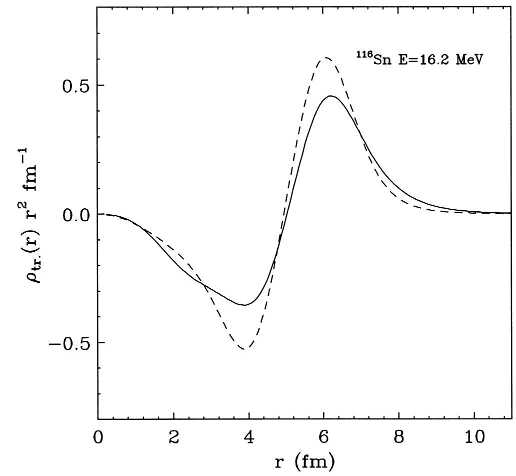

Fig. 2. Microscopic RPA (solid line) and collective model (dashed line) transition densities in ^{116}Sn at the resonance energy $E = 16.2$ MeV.

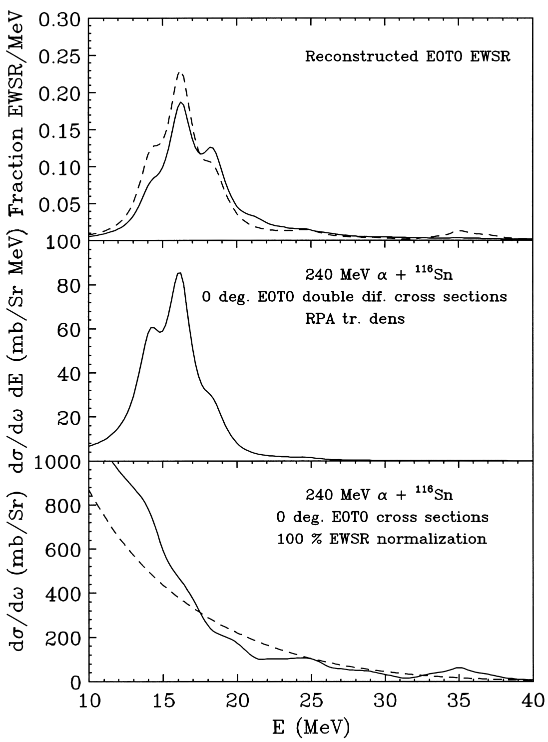

Fig. 3. Reconstruction of the ISGMR EWSR from 0 degree cross sections. Solid line: results obtained using RPA transition density. Dashed line: results obtained using collective model transition density. See text for a detailed explanation of the figure.

fraction of the E0T0 EWSR per unit energy as calculated from the E0T0 transition strength distribution of Fig. 1.

The described calculations provide a direct test of approximation (9). If the collective model shape (9) of the E0T0 transition density exactly reproduced the microscopic shape deduced from Eq. (5), the solid and dashed curves in the upper panel of Fig. 3 would coincide. However, as follows from our calculations, the differences between the actual (RPA) strength distributions and those reconstructed from the cross section spectrum are noticeable. Moreover, these differences are not uniform which could result in differences between the E0T0 centroid energies calculated from the actual E0T0 strength distribution and the reconstructed one. In Table 2 we display amounts of the total E0T0 EWSR exhausted by the actual (RPA) and the reconstructed E0T0 strength distributions within the considered energy interval. The comparison of the E0T0 centroid energies calculated from the actual and reconstructed E0T0 strength distributions is presented in Table 3. It can be seen that the cross section analysis based on approximation (9) tends to overestimate the E0T0 EWSR and the percentage of such an overestimation becomes larger for lighter nuclei. Approximation (9) also results in the shift of the E0T0 centroid energies, however, as follows from our results, this error does not exceed 2%.

Table 2. Percentages of the E0T0 EWSR exhausted by the RPA strength distribution and the one reconstructed from 0 degree cross sections following the procedure described in text.

Nucleus	Energy range (MeV)	Actual (RPA) (%)	Reconstructed (%)
^{28}Si	10÷40	91	113
^{40}Ca	10÷40	94	114
^{58}Ni	10÷40	96	113
^{116}Sn	10÷40	95	106

Table 3. Centroid energies (in MeV) obtained from the RPA strength distribution and the one reconstructed from 0 degree cross sections.

Nucleus	Energy range (MeV)	$\frac{M_1}{M_0}$ (RPA)	$\frac{M_1}{M_0}$ (Reconstructed)	% difference
^{28}Si	10÷40	24.0	24.5	2.1
^{40}Ca	10÷40	21.1	21.3	0.9
^{58}Ni	10÷40	21.2	20.8	1.4
^{116}Sn	10÷40	17.2	16.8	2.3

Conclusions

By performing self-consistent Hartree-Fock-RPA calculations, we provided a microscopic description of isoscalar monopole excitations in several nuclei ranging from ^{28}Si to ^{116}Sn. Our results were compared with recent experimental data. Good agreement with the experiment was obtained for ^{28}Si and ^{40}Ca. While recent studies of 240 MeV α + ^{58}Ni reaction were unable to locate more than 50% of the E0T0 EWSR in ^{58}Ni, our microscopic calculations showed that almost the entire E0T0 strength in this nucleus is located in the energy region $E < 40$ MeV.

Using the density dependent Gaussian form (7) of the nucleon-α interaction and the folding model DWBA, we gave a theoretical description of 240 MeV α-particle scattering by ^{28}Si, ^{40}Ca, ^{58}Ni and ^{116}Sn targets. Experimentally measured elastic angular distributions were nicely reproduced by the parametrization of the nucleon-α interaction given in Eq. (11).

We tested the approximation of the E0T0 transition density by the collective model result (9). Our results, which were obtained by following closely the typical experimental procedure, showed that the analysis of E0T0 inelastic cross sections based on the approximation (9) tends to overestimate the E0T0 EWSR by up to 20% (which agrees with conclusions of Ref. 11) and shifts the E0T0 centroid energies by up to 2%. These conclusions may be important for further experimental studies of E0T0 excitation, especially in light nuclei. Possible overestimation of the E0T0 EWSR in the experimental analysis of cross sections makes the problem of missing monopole strength in ^{58}Ni even worse. Further theoretical and experimental efforts are, thus, necessary to resolve this problem.

This work was supported in part by the US Department of Energy under grant # FG03-93ER40773.

References

1) A. Bohr and B. R. Mottelson: *Nuclear Structure*, Vol. 2, Chap. 6 (W. A. Benjamin, London, 1975).
2) N. K. Glendenning: Phys. Rev. C **37**, 2733 (1988).
3) J. P. Blaizot, D. Gogny, and B. Grammaticos: Nucl. Phys. A **265**, 315 (1976).
4) J. P. Blaizot: Phys. Rep. **64**, 171 (1980).
5) J. P. Blaizot, J. F. Berger, J. Decharge, and M. Girod: Nucl. Phys. A **591**, 435 (1995).
6) J. Treiner, H. Krivne, O. Bohigas, and J. Martorell: Nucl. Phys. A **371**, 253 (1981).
7) D. H. Youngblood, H. L. Clark, and Y.-W. Lui: Phys. Rev. C **76**, 1429 (1996).
8) D. H. Youngblood, Y.-W. Lui, and H. L. Clark: Phys. Rev. C **55**, 2811 (1997).
9) D. H. Youngblood, H. L. Clark, and Y.-W. Lui: Phys. Rev. C **57**, 1134 (1998).
10) D. H. Youngblood, Y.-W. Lui, and H. L. Clark: Phys. Rev. C **57**, 2748 (1998).
11) P. Chomas, T. Suomijarvi, N. Van Giai, and J. Treiner: Phys. Lett. B **281**, 6 (1992).
12) K.-F. Liu, H. Luo, Z. Ma, and Q. Shen: Nucl. Phys. A **534**, 1 (1991).
13) G. F. Bertsch and S. F. Tsai: Phys. Rep. **18**, 125 (1975).
14) J. Bar Touv, A. Moalem, and S. Shlomo: Nucl. Phys. A **339**, 303 (1980).
15) S. F. Tsai: Phys. Rev. C **17**, 1862 (1978).
16) K. F. Liu, H. Luo, Z. Ma, and Q. Shen: Nucl. Phys. A **534**, 25 (1991).
17) D. J. Thouless: Nucl. Phys. **22**, 78 (1961).
18) G. R. Satchler and W. G. Love: Phys. Rep. **55**, 183 (1979).
19) G. R. Satchler: *Direct Nuclear Reactions* (Oxford University Press, Oxford, 1983).
20) D. J. Horen, J. R. Beene, and G. R. Satchler: Phys. Rev. C **52**, 1554 (1995).
21) J. R. Beene, D. J. Horen, and G. R. Satchler: Phys. Lett. B **344**, 67 (1995).
22) G. R. Satchler and D. T. Khoa: Phys. Rev. C **55**, 285 (1997).
23) H. L. Clark, Y. -W. Lui, and D. H. Youngblood: Phys. Rev. C **57**, 2887 (1998).
24) G. R. Satchler: Nucl. Phys. A **472,** 215 (1987).
25) M. Rhoades-Brown et al.: Phys. Rev. C **21**, 2417 (1980); M. H. Macfarlane and S. C. Pieper: Argonne National Laboratory Report, No. ANL-76-11, Rev. 1 (1978), unpublished.
26) S. Brandenburg, R. De Leo, A. G. Drentje, M. N. Harakeh, H. Sakai, and A. van der Woude: Phys. Lett. B **130**, 9 (1983).